

Model-based Loss Minimization Control of a Squirrel cage Induction Motor Drive with shorted Rotor under Indirect Field Orientation

Ayobami Olajube, Olugbenga Moses Anubi

Department of Electrical and Computer Engineering, FAMU-FSU College of Engineering
Center for Advanced Power Systems, Florida State University
E-mail: {aao21b, oanubi}@fsu.edu

Abstract—This paper presents the development of an energy saving scheme via indirect field oriented control (IFOC) at the optimum operating region. A model-based steady state power loss analysis is carried out to determine the optimal speed and the optimal rotor flux that will serve as reference for the speed and torque tracking control. IFOC ensures the decoupled control of the torque and flux components of the stator current in a similar version as in DC drives through rotor flux orientation. The need for multiple sensors is eliminated by the analytical loss model approach, leading to an appreciable cost reduction. PI controller is used for the independent control of the flux and the torque producing components of the stator current. This is done at steady state, using the optimal rotor flux and speed computed in a loss minimization algorithm. The gains for optimum performance of the PI controller is selected via genetic algorithm (GA) optimization technique. The developed scheme is validated via a realistic numerical simulation and, the shorted rotor induction machine shows a very efficient speed and torque tracking performance at various load conditions and speed settings.

Index Terms—vector control, indirect field orientation, PI controller, optimum rotor flux, optimum speed, GA-tuned PI controller, shorted-rotor induction machine, optimization, power loss

I. INTRODUCTION

Astronomical rise in the energy consumption of the electric drives such as the induction motors in the domestic, commercial and industrial applications has had a very strong impact on the utility grids all over the world. This has necessitated the need to improve the efficiency of these drives by invariably lowering the losses and costs. Electric drives are responsible for about 60% of the electric energy consumed in the industries worldwide [1] [2]. Hence, improving the efficiency will definitely provide energy savings and cost conservation. The most popular method of flux control for efficiency improvement in the industrial drives is the vector control also known as the field-oriented control [3]–[5]. In literature, there are three categories of control methods that have been used mainly to achieve improved drive efficiency [6]. They are the simple state control (SSC) [7], loss model control (LMC) [8] [9] and the search control (SC) techniques [10]–[12]. LMC is the fastest approach that involves the use of machine model to compute the losses by selecting appropriate value of flux that minimizes these losses. The method has been found to be limited by parameter variations. SSC on the other hand is the simple version of LMC

through the use of state space control technique which may include observer design to estimate the value of the required flux for cost and loss minimization [13]. SC method is highly insensitive to parameter variations but suffers from slow convergence and torque ripples [1] [3] [4], [14], [15]. Fuzzy logic control method has been proposed to encourage fast convergence of search control technique and prevent torque ripples [16]. Neuro-fuzzy method was also proposed to improve on the fuzzy logic technique. These proposed methods are insensitive to parameter variations and are easy to implement than the actual SC method [17] [18] [19]. The PID controller is commonly used in the industry to control IM but parameter sensitivity, speed and load disturbances have limited its effectiveness. Thus, adaptive controllers such as the model reference systems control technique have recently been utilized at high level [20] [21].

This paper presents a PI-based indirect field-oriented control of a shorted rotor induction motor to achieve loss minimization at steady state in an optimum operating regime using jacobi matrix. The key contributions in this article are:

- 1) The derivation of a unique model-based power loss and the efficiency equations for the squirrel cage induction motor with shorted rotor.
- 2) Determination of the optimal rotor speed and flux using jacobi matrix at steady state [22].
- 3) The use of genetic algorithm (GA) technique to tune the PI to select the best control gains for the PI controller to ensure optimum performance.

The rest of the paper is organised as follows: section II shows the notation of the machine parameters and other variables, section III shows the induction machine dynamic model development, section IV depicts the indirect field-oriented control formulation, section V enumerates the steady state power loss model derivation, section VI shows the PI controller design, section VII shows results description and the conclusion is shown in section VIII.

II. NOTATIONS

r_s, r_r stator and rotor resistances as referred

r_c core loss resistance as referred

p, L_m number of poles and magnetizing inductance

L_{ls}, L_{lr} stator and rotor self inductances as referred

$L_s = L_{ls} + L_m$ stator leakage inductances as referred

$L_r = L_{lr} + L_m$ rotor leakage inductances as referred

$\lambda_{ds}, \lambda_{qs}$ d and q axes stator fluxes
 $\lambda_{dr}, \lambda_{qr}$ d and q axes rotor fluxes
 I_{ds}, I_{qs} d and q axes stator currents
 I_{dr}, I_{qr} d and q axes rotor currents
 V_{ds}, V_{qs} d and q axes stator voltages
 V_{dr}, V_{qr} d and q axes rotor voltages
 I_{ds}^*, I_{qs}^* computed d and q axes stator current references
 T_{em} generated electromagnetic torque
 T_m load torque
 $s, \omega_{s0} = \omega - \omega_r$ Slip and Slip frequency
 $\omega = \frac{d\theta}{dt}$ stator speed at rated frequency
 $\omega_r = \frac{d\theta_r}{dt}, \omega_m$ rotor and mechanical speeds
 H is the equivalent inertia as referred to the stator
 τ_r is the rotor flux time constant

III. INDUCTION MACHINE DYNAMIC MODEL

The circuits in Fig.1 show the simplified equivalent circuit model of a 3-phase, symmetrical squirrel-cage induction motor in a d-q synchronous reference frame with core loss.

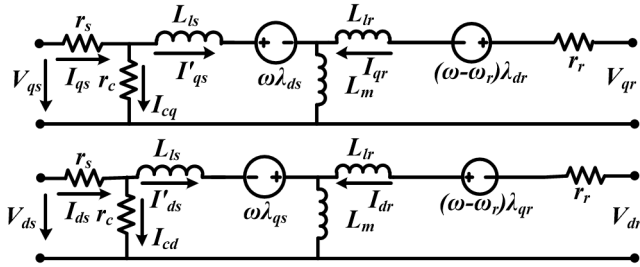


Fig. 1: d-q axes circuit equivalent of an IM

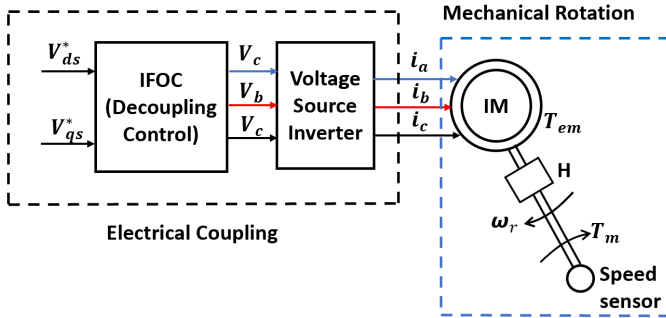


Fig. 2: Electrical coupling with mechanical rotation in IM

The dynamical model of the induction machine derived from Fig.1 is given by:

$$\begin{aligned}
 V_{ds} &= r_s I_{ds} - \omega \lambda_{ds} + \frac{d\lambda_{qs}}{dt} \\
 V_{qs} &= r_s I_{qs} + \omega \lambda_{qs} + \frac{d\lambda_{ds}}{dt} \\
 V_{dr} &= r_r I_{dr} - \omega_{s0} \lambda_{dr} + \frac{d\lambda_{qr}}{dt} \\
 V_{qr} &= r_r I_{qr} + \omega_{s0} \lambda_{qr} + \frac{d\lambda_{dr}}{dt}
 \end{aligned} \quad (1)$$

Moreover, the flux linkage for a magnetically linear drive is given in terms of the reference frame currents as [23]:

$$\begin{bmatrix} \lambda_{ds} \\ \lambda_{qs} \\ \lambda_{dr} \\ \lambda_{qr} \end{bmatrix} = \begin{bmatrix} L_s & 0 & L_m & 0 \\ 0 & L_s & 0 & L_m \\ L_m & 0 & L_r & 0 \\ 0 & L_m & 0 & L_r \end{bmatrix} \begin{bmatrix} I_{ds} \\ I_{qs} \\ I_{dr} \\ I_{qr} \end{bmatrix} \quad (2)$$

Using (1) and (2) with the assumption that the rotor of the machine is shorted ($V_{dr} = V_{qr} = 0$). Thus, the dynamic of the drive is summarized as:

$$\begin{bmatrix} \dot{\lambda}_{ds} \\ \dot{\lambda}_{qs} \\ \dot{\lambda}_{dr} \\ \dot{\lambda}_{qr} \end{bmatrix} = F \begin{bmatrix} \lambda_{ds} \\ \lambda_{qs} \\ \lambda_{dr} \\ \lambda_{qr} \end{bmatrix} + N \begin{bmatrix} I_{ds} \\ I_{qs} \\ I_{dr} \\ I_{qr} \end{bmatrix} + \begin{bmatrix} V_{ds} \\ V_{qs} \\ 0 \\ 0 \end{bmatrix} \quad (3)$$

where the resistive matrix N is given by $N = \text{diag}(r_s, r_s, r_r, r_r)$ and

$$F = \begin{bmatrix} 0 & \omega & 0 & 0 \\ -\omega & 0 & 0 & 0 \\ 0 & \omega_{s0} & 0 & 0 \\ -\omega_{s0} & 0 & 0 & 0 \end{bmatrix}$$

The electrical coupling with the mechanical rotation of the drive containing the inertia, load torque, electromagnetic torque and the rotor speed shown in Fig.2 is expressed as:

$$\frac{d\omega_r}{dt} = \frac{p}{2H} (T_{em} - T_m) \quad (4)$$

where the electromagnetic torque T_{em} is the cross product of the stator d-q and the rotor d-q current vectors.

$$T_{em} = \frac{3p}{4} L_m (I_{dqs} \times I_{dqr}) \quad (5)$$

$$T_{em} = \frac{3p}{4} L_m (I_{dqs}^T J I_{dqr})$$

where $I_{dqs} = \begin{bmatrix} I_{ds} \\ I_{qs} \end{bmatrix}$, $I_{dqr} = \begin{bmatrix} I_{dr} \\ I_{qr} \end{bmatrix}$ and $J = \begin{bmatrix} 0 & -1 \\ 1 & 0 \end{bmatrix}$. T_{em} from (5) is rewritten in a more familiar form as:

$$T_{em} = \frac{3p}{4} L_m (I_{qs} I_{dr} - I_{ds} I_{qr}) \quad (6)$$

Then, the steady state initial conditions for the drive are computed by turning the derivative terms in (3) and (4) to zero. In the next section, an indirect field-oriented control scheme will be formulated to develop the controller required for the drive.

IV. INDIRECT FIELD-ORIENTED CONTROL FORMULATION

In the IFOC of Induction machine, the rotor flux is aligned onto d-axis of the synchronous reference frame as follows:

$$\lambda_r = \lambda_{dr}, \lambda_{qr} = \sqrt{\lambda_r^2 - \lambda_{dr}^2} = 0 \text{ and } \dot{\lambda}_{qr} = 0$$

From (1) and (2);

$$I_{qr} = -\frac{L_m}{L_r} \cdot I_{qr} \quad (7)$$

$$I_{dr} = \frac{\lambda_{dr} - L_m I_{ds}}{L_r} \quad (8)$$

$$(\omega - \omega_r) = \frac{r_r L_m}{L_r} \cdot \frac{I_{qs}}{\lambda_{dr}} \quad (9)$$

$$\dot{\lambda}_{dr} + \frac{r_r}{L_r} \lambda_{dr} = \frac{r_r L_m}{L_r} \cdot I_{ds} \quad (10)$$

$$\lambda_{dr} = \lambda_r = \frac{L_m I_{ds}}{1 + s\tau_r} \quad (11)$$

where $\tau_r = \frac{L_r}{r_r}$ is the rotor time constant.

$$I_{qs}^* = \frac{T_{em}}{K_e \lambda_r} \quad (12)$$

$$I_{ds}^* = \frac{|\lambda_{r_{opt}}|}{L_m} \quad (13)$$

Then, the desired torque dependent component of the stator current is computed from (12), where $K_e = \frac{3pL_m}{4L_r}$. And the estimated flux dependent component of the stator current I_{ds}^* is computed from (13) by using the optimum flux $|\lambda_{r_{opt}}|$ derived in section V, which serves as the reference input flux.

The indirect vector control setting is designed as follows:

$$L_\sigma \dot{I}_{qs} + r I_{qs} = V_{qs} - \omega L_\sigma I_{ds} - \frac{\omega_r L_m}{L_r} \cdot \lambda_{dr} \quad (14)$$

$$L_\sigma \dot{I}_{ds} + r I_{ds} = V_{ds} + \omega L_\sigma I_{qs} + \frac{r_r L_m}{L_r^2} \cdot \lambda_{dr} \quad (15)$$

$$\sigma_{qs} = L_\sigma \dot{I}_{qs} + r I_{qs} = K (I_{qs}^* - I_{qs}) \quad (16)$$

$$\sigma_{ds} = L_\sigma \dot{I}_{ds} + r I_{ds} = K (I_{ds}^* - I_{ds}) \quad (17)$$

$$I_{qs}^* - I_{qs} = I_{ds}^* - I_{ds} = e \quad (18)$$

Where K can be any controller, σ_{ds} and σ_{qs} are the controller outputs, I_{qs}^* and I_{ds}^* are the desired q and d axes currents, and $L_\sigma = L_s - \frac{L_m^2}{L_r}$ is the stator leakage factor. The controller error 'e' is shown in (18).

Using the PI controller and the carrier-based pulse-width modulation scheme:

$$K = K_p + \frac{K_i}{s} \quad (19)$$

$$M_{qs} = \frac{2V_{qs}}{V_{dc}} \quad (20)$$

$$M_{ds} = \frac{2V_{ds}}{V_{dc}} \quad (21)$$

Where K_p is the proportional gain, K_i is the integral gain, M_{qs} is the inverter modulation index for q-axis and M_{ds} is the d-axis modulation index. Then the inner control loop equations of the drive with desired q and d axes currents I_{qs}^* and I_{ds}^* are given as;

$$K (I_{qs}^* - I_{qs}) = V_{qs} - \omega L_\sigma I_{ds} - \frac{\omega_r L_m}{L_r} \cdot \lambda_{dr} \quad (22)$$

$$K (I_{ds}^* - I_{ds}) = V_{ds} + \omega L_\sigma I_{qs} + \frac{r_r L_m}{L_r^2} \cdot \lambda_{dr} \quad (23)$$

Coupling (20), (21) (22) and (23), the equation for the inner loop control is developed as shown in Fig.3 as;

$$M_{qs} = K (I_{qs}^* - I_{qs}) + \omega L_\sigma I_{ds} + \frac{\omega_r L_m}{L_r} \cdot \lambda_{dr} \quad (24)$$

$$M_{ds} = K (I_{ds}^* - I_{ds}) - \omega L_\sigma I_{qs} - \frac{r_r L_m}{L_r^2} \cdot \lambda_{dr} \quad (25)$$

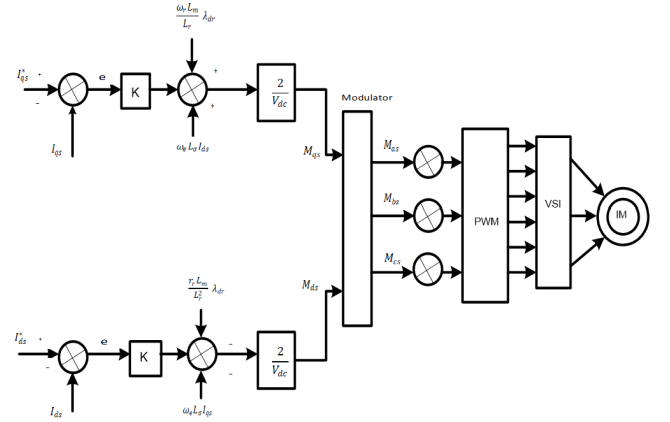


Fig. 3: Inner loop current control

The next section is dedicated to the power loss equation development from Fig.1.

V. MODEL-BASED ELECTRICAL POWER LOSS FORMULATION AT STEADY STATE

The practical assumption here is that no loss minimization exist during torque transients which helps to reduce the problem of poor torque response due to low flux [1]. With this in mind, we develop the core loss current I_c and the stator current I_s from Fig.1 as:

$$I_c^2 = I_{qc}^2 + I_{dc}^2 \quad (26)$$

$$I_c^2 = \frac{L_s I_r^2}{(\omega - \omega_r)^2 L_m^2} \left\{ r_r^2 + (\omega - \omega_r)^2 L_r^2 \right\} - 2L_s L_r I_r^2 + L_m^2 I_r^2 \quad (27)$$

$$I_s^2 = \left[\frac{1}{(\omega - \omega_r)^2 L_m^2} \left\{ r_r^2 + (\omega - \omega_r)^2 L_r^2 \right\} (1 + L_s^2) + \frac{2\omega r_r}{r_c (\omega - \omega_r)} - 2L_s L_r + L_m^2 I_r^2 \right] \quad (28)$$

A. Steady State Power Loss and Torque Formulation

The total power loss equation for the drive at steady state is shown in (31) below:

$$P_L = \frac{3}{2} (I_s^2 r_s + I_r^2 r_r + I_c^2 r_c) \quad (29)$$

By substituting the expressions derived above for the stator and core loss currents in (27) and (28) into (29), we arrive

at the a more expansive form shown in (30). Then, the corresponding steady state electromagnetic torque in d-q reference frame is also derived as shown in (31):

$$P_L = \frac{3}{2} I_r^2 \left(\alpha + \frac{\beta \omega}{(\omega - \omega_r)} + \frac{\gamma}{(\omega - \omega_r)^2} \right) \quad (30)$$

Where,

$$\alpha = r_r + (r_s + r_c) (L_m^2 - 2L_s L_r) + \frac{L_r^2}{L_m^2} (r_s + (r_s + r_c) L_s^2), \beta = \frac{2r_r r_s}{r_c}, \text{ and}$$

$$\gamma = \frac{r_r^2}{L_m^2} (r_s + (r_s + r_c) L_s^2).$$

$$T_{em} = T_m = \frac{3p}{4} (\lambda_{qr} I_{dr} - \lambda_{dr} I_{qr}) = \frac{3pr_r}{4(\omega - \omega_r)} I_r^2 \quad (31)$$

Combining (30) and (31), the power loss equation in terms of the electromagnetic torque at steady state is derived as:

$$P_L = \frac{2T_m}{pr_r} \left(\alpha (\omega - \omega_r) + \beta \omega + \frac{\gamma}{(\omega - \omega_r)} \right) \quad (32)$$

The variation of the power loss with respect to the rotor flux is formulated as shown in (33);

$$P_L = \zeta \lambda_r^2 + \frac{\mu T_m^2}{\lambda_r^2} \quad (33)$$

where $\zeta = \frac{r_s + r_c}{L_m^2}$ and $\mu = \frac{r_s L_r^2 + r_r L_m^2 + L_r(L_r - L_m)r_c}{p^2 L_m^2}$.

Then, the optimum efficiency of the drive is derived as:

$$\eta = \frac{2400\lambda_r^2}{2400\lambda_r^2 + \zeta\lambda_r^4 + \mu T_m^2} \quad (34)$$

B. Model-based Power Loss Minimization

A second order jacobi matrix in (35) is used to solve an optimization problem formulated from (30) and (31), to obtain the lowest power loss corresponding to the minimization of the torque and output power of the induction motor. The solution gives a steady state optimal slip frequency at which the machine will run at the highest efficiency corresponding to the lowest power loss [22].

$$\begin{vmatrix} \frac{dP_L}{d\omega} & \frac{dP_L}{dI_r} \\ \frac{dT_m}{d\omega} & \frac{dT_m}{dI_r} \end{vmatrix} = 0 \quad (35)$$

Solving (35) gives the optimal speed at which the machine will run and the optimal flux as functions of the machine parameters as:

$$\omega_{opt} - \omega_r = \pm \sqrt{\frac{\gamma}{\alpha + \beta}} \quad (36)$$

$$|\lambda_{r_{opt}}| = \sqrt{\frac{4r_r T_m}{3p} \sqrt{\frac{\alpha + \beta}{\gamma}}} \quad (37)$$

The computed values in (36) and (37) are used as references for the speed tracking and torque trajectory control.

Hence, the flux dependent component of the stator current I_{ds}^* shown in (13) is computed, and the desired torque corresponding to the highest efficiency is determined at steady state.

TABLE I: shorted rotor induction machine parameters [24]

Parameters	Value
Rated Power, P	2.4KW at 0.8pf
Rated Voltage (L-L, rms)	460 V
frequency	60 Hz
Speed at 60 Hz	1800rpm
Rotor speed, ω	1750rpm
Rated slip, s	1.77%
Full-load current, I	4 A
number of poles, p	4
Machine inertia, H	0.025 kg/m ²
Efficiency, η	88.5%
Stator resistance, r_s	1.77 Ω
Rotor resistance, r_r	1.34 Ω
Core loss resistance, r_c	1200 Ω
Stator leakage inductance, L_s	0.383H
Rotor self leakage inductance, L_r	0.381H
mutual inductance, L_m	0.369H

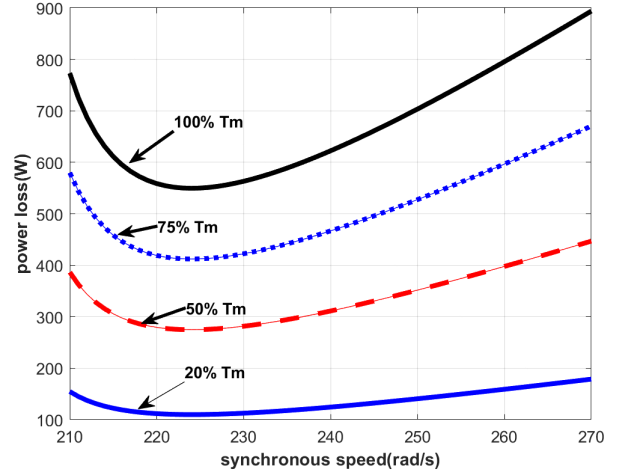


Fig. 4: Minimized steady state power losses at different loads

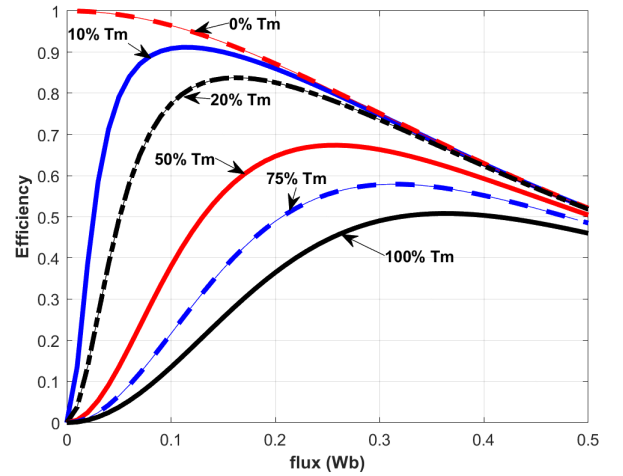


Fig. 5: Variation of efficiency with rotor flux at different load torques

VI. PI CONTROLLER DESIGN FOR THE DRIVE

According to (20)-(25), a carrier-based PWM voltage source inverter is used to switch the induction motor through

the independent control of the flux component and the torque producing component of the stator current as shown in Fig.6. The angle obtained from the estimated drive is fed back for rotor orientation in the IFOC block and the estimated torque is also computed which can be compared with generated electromagnetic torque from the actual drive. The speed and the electromagnetic torque profiles are examined for PI-controlled IM drive at various changes in load and parameter variations.

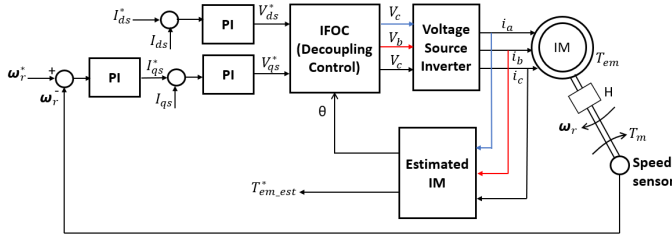


Fig. 6: IFO Control of an Induction Motor

The PI involves selecting specific gains K_p for the proportional and K_i for the integral components to achieve both the speed and flux regulation at the highest possible torque. The inputs to the controllers are the errors generated from comparing the flux-dependent currents I_{ds}^* computed using the optimal flux from the power loss minimization model and the I_{ds} of the IM drive. The speed is also independently regulated to generate error that produce the torque dependent stator current I_{qs}^* through a PI controller. The current is then compared to I_{qs} obtained from the IM drive, to give an error that is passed through another PI controller to produce a control signal for the drive. The performance of the controller is further optimized by using GA to choose the best possible K_p and K_i values.

The PI controller used for the flux dependent stator current control is of the form;

$$I_{ds} = I_{ds}^* - K_p V_{ds}^* - K_i \int_0^t V_{ds}^*(\tau) d\tau \quad (38)$$

In addition to (38), the inner and the outer loop PI controllers for the torque-dependent component of the stator current are given as (39) and (40) respectively;

$$I_{qs} = I_{qs}^* - K_p V_{qs}^* - K_i \int_0^t V_{qs}^*(\tau) d\tau \quad (39)$$

$$\omega_r = \omega_r^* - K_p I_{qs}^* - K_i \int_0^t I_{qs}^*(\tau) d\tau \quad (40)$$

Where $I_{ds}^* \geq 0$, $I_{qs}^* \geq 0$, $V_{ds}^* \geq 0$, $V_{qs}^* \geq 0$, $\omega_r^* \geq 0$ are the control references and K_p , K_i are the controller gains.

VII. RESULTS AND DISCUSSION

Fig.4 shows the power losses determined at the optimum speed of 225 rad/sec for different loads. The corresponding rotor flux at the optimal operating region is approximately 208 rad/sec , which is taken as the reference to the torque trajectory controller. Then, the optimum flux at the rated

torque of the drive in Table I is $|\lambda_{r_{opt}}| = 0.323 \text{ Wb}$ and it is taken as the reference to the flux-dependent load current controller. The higher the developed mechanical torque, the higher the losses at a constant optimal speed. Hence, the torque is maintained at a low value by ensuring a low magnitude of the optimal flux.

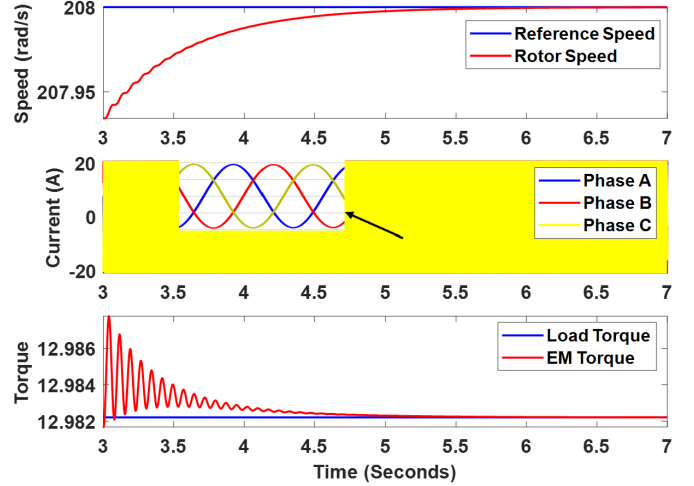


Fig. 7: Constant speed reference, phase currents, torque response

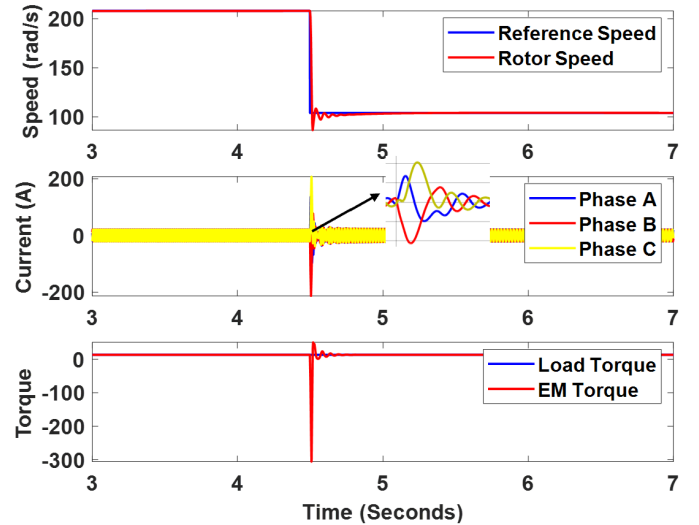


Fig. 8: Step Rotor speed reference speed tracking, phase currents and Torque response at a constant load

Similarly, Fig.5 shows that the highest efficiency is 100 percent at zero load torque and obviously decreasing with increase in load. The implication of this is that loss minimization is generally possible with vector control at light loads but more difficult as the load increases. Different optimal flux values occur at different loads and the efficiency of the drive reach over 90 percent at a load torque of 10 percent. At 20 percent load torque, the efficiency is below 90 percent.

Hence, the optimal flux doesn't essentially guarantee an improved drive performance. The possibility of an improved

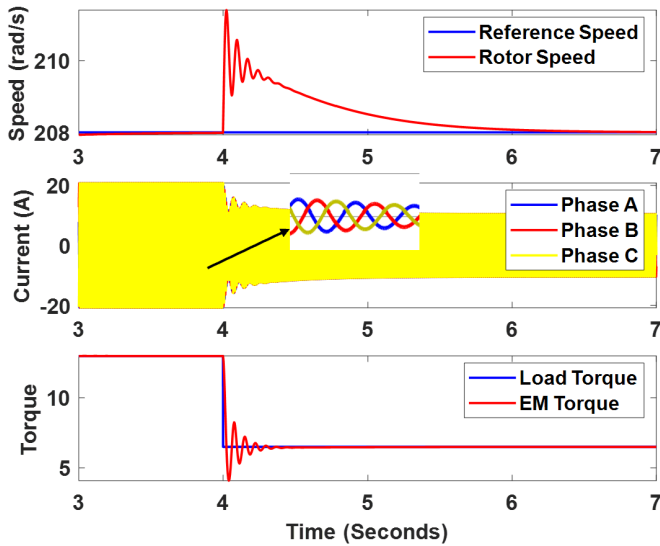


Fig. 9: constant Rotor speed reference speed tracking, phase currents and Torque response at a step load

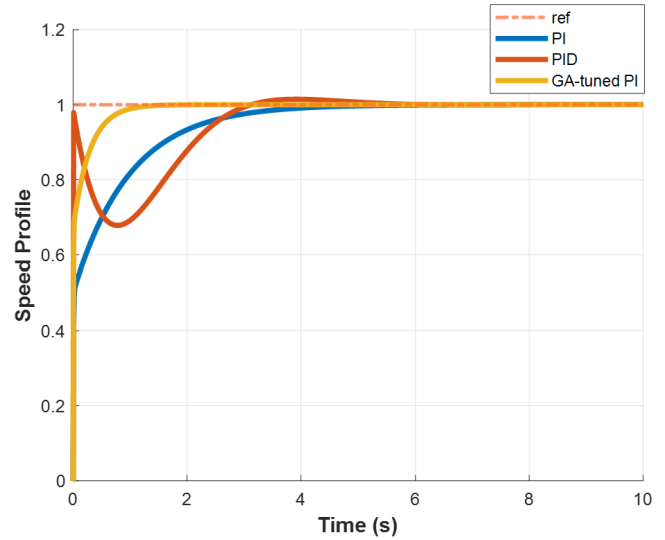


Fig. 11: Performance comparison between PI, PID and GA-tuned PI controllers

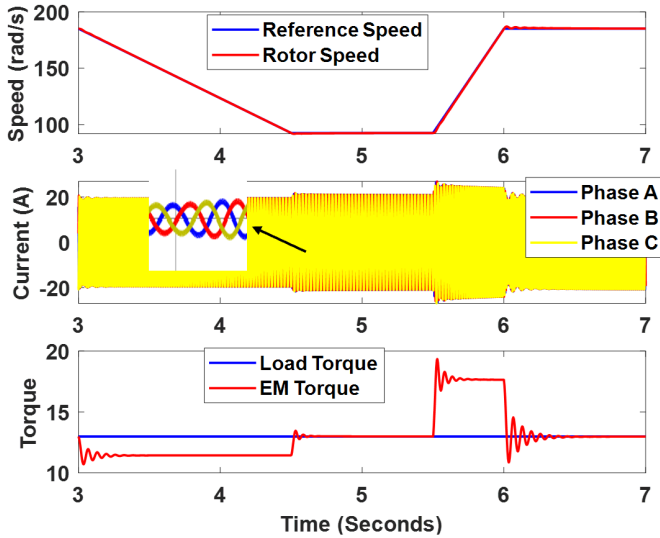


Fig. 10: Drive cycle reference speed tracking, phase currents and Torque response at a constant load

TABLE II: Comparative Performance Analysis on Speed Trajectory

Method	Jacobi-PI	GA-PI	PID
<i>Computation</i>	Fastest	Slower	Faster
<i>Implementation</i>	Simplest	Complex	Simpler
<i>Torque ripple</i>	Lower	Lowest	Highest
<i>Overshoot</i>	0%	0%	3.07%
<i>Settling time</i>	6 secs	1.5 secs	6 secs
<i>Rise time</i>	1.47 secs	0.31 secs	2.14 secs
<i>Parameter requirement</i>	τ_r	none	τ_r
<i>Parameter Sensitivity</i>	Yes	None	yes

performance is only possible at the lowest load torques leading to a very small magnitude of rotor fluxes which

must be kept within certain limits to prevent magnetic field saturation. The power loss of the voltage-source PWM inverter is not considered because both the conduction and switching losses are negligible, especially in larger drives [24]. Fig.7 shows the behaviour of the drive at a constant reference speed and a constant load. The rotor speed tracks the reference perfectly at a very low steady state error. The generated electromagnetic torque also follows the speed and tracks the load torque appropriately. That is, the drive has a good speed regulation at constant load.

Furthermore, the response of the drive to a step speed at constant load is shown in Fig.8. When the reference speed drops to half its initial value at 4secs. The rotor speed tracks the reference trajectory perfectly while torque dips sharply at 4secs before returning to steady state almost immediately. This indicates the sensitivity of PI controller to parameter variation. Nonetheless, the speed regulation and torque response remains good under this scenario. Fig.9 shows the speed and torque response to a constant reference speed at step load torque. After a step of 4secs, the speed rises sharply while the torque dips accordingly before steady state is reached quickly. In most of the simulation results, the response settles to a steady state around 6secs, which can be considered relatively fast at the practically considerable controller gain values.

Additionally, a speed profile reference response is shown in Fig.10, in which a drive cycle reference is used to test the robustness of the PI-controllers against the rapidly changing speed in electric vehicle applications. The rotor speed tracks the reference accordingly despite the ramp-drop in speed and this continues throughout the trajectory. However, the torque experience initial pulsations with respect to the drop in speed. It has perfect tracking only within steady speed profile between 4.5 to 5.5secs. But, the response settles faster with increase in the PI-controller gains to give a desirable speed

regulation and torque performance. The proposed Jacobi-PI method exhibit a good performance as shown in Table II. The response reaches steady state faster When the PI-controller is tuned with GA. its settling time improve from 6secs to 1.5secs. When compared with PID within speed tracking trajectory, it doesn't have any overshoot and the rise time is also lower. Its sensitivity to parameter variation is improved when optimized with GA as studied in [25]. Although, the proposed method depends on the rotor time constant τ_r , unlike the case in GA-tuned PI [26] [27], yet the computation time of the latter is longer. However, GA-PI exhibits fastest response but can be costlier to experiment.

VIII. CONCLUSION

A model-based loss minimization is proposed for a squirrel cage shorted rotor induction machine without due consideration for the torque transient characteristics. Nonlinearities in the machine dynamics often require complex optimization methods to estimate the optimal operating region of the drives online, which may eventually drive up the cost of the machine. However, in this article, a simple Jacobi minimization technique is used for the power loss minimization at steady state to extract the optimal speed and the optimal flux for the drive at the best possible torque. This algorithm guarantees cost reduction and ensure considerable power loss reduction leading to higher operational efficiency. A defacto control method for the electric drives in the industries known as the field-oriented control is used to ensure the decoupled control of the torque-producing and the flux-producing components for the stator current through indirect rotor orientation. In addition, practically simple PI controllers are used to ensure good speed regulation and torque trajectory. The performance of the controller is enhanced by using GA to select optimal gain values. The results show a cost conserving, high performing drive with a very low power loss especially at a very low torque and rotor flux. Nonetheless, it has limitations under transient performance characteristics when compared with other superior numerical optimization algorithms.

REFERENCES

- [1] J.-F. Stumper, A. Dötlinger, and R. Kennel, "Loss minimization of induction machines in dynamic operation," *IEEE transactions on energy conversion*, vol. 28, no. 3, pp. 726–735, 2013.
- [2] D. S. Kirschen, D. W. Novotny, and T. A. Lipo, "Optimal efficiency control of an induction motor drive," *IEEE Transactions on Energy Conversion*, no. 1, pp. 70–76, 1987.
- [3] C. Chakraborty and Y. Hori, "Fast efficiency optimization techniques for the indirect vector-controlled induction motor drives," *IEEE Transactions on Industry Applications*, vol. 39, no. 4, pp. 1070–1076, 2003.
- [4] C. Chakraborty, M. C. Ta, and T. Hori, "Speed sensorless, efficiency optimized control of induction motor drives suitable for ev applications," in *IECON'03. 29th Annual Conference of the IEEE Industrial Electronics Society (IEEE Cat. No. 03CH37468)*, vol. 1. IEEE, 2003, pp. 913–918.
- [5] J. Moreno-Eguilaz and J. Peracaula, "Efficiency optimization for induction motor drives: past, present and future," in *Electrimacs 99 (modelling and simulation of electric machines converters and systems)*, 1999, pp. 1–187.
- [6] F. Abrahamsen, J. K. Pedersen, and F. Blaabjerg, "State-of-the-art of optimal efficiency control of induction motor drives," in *State-of-the-Art of Optimal Efficiency Control of Induction Motor Drives*. i Forlag uden navn, 1996, pp. 163–170.
- [7] C. Lascu and A. M. Trzynadlowski, "Combining the principles of sliding mode, direct torque control, and space-vector modulation in a high-performance sensorless ac drive," *IEEE Transactions on industry applications*, vol. 40, no. 1, pp. 170–177, 2004.
- [8] M. N. Uddin and S. W. Nam, "Development of a nonlinear and model-based online loss minimization control of an im drive," *IEEE Transactions on energy conversion*, vol. 23, no. 4, pp. 1015–1024, 2008.
- [9] M. N. Uddin, M. M. Rahman, B. Patel, and B. Venkatesh, "Performance of a loss model based nonlinear controller for ipmsm drive incorporating parameter uncertainties," *IEEE Transactions on Power Electronics*, vol. 34, no. 6, pp. 5684–5696, 2018.
- [10] H.-u. Rehman and L. Xu, "Alternative energy vehicles drive system: Control, flux and torque estimation, and efficiency optimization," *IEEE Transactions on Vehicular Technology*, vol. 60, no. 8, pp. 3625–3634, 2011.
- [11] D. Kastha and B. K. Bose, "On-line search based pulsating torque compensation of a fault mode single-phase variable frequency induction motor drive," *IEEE transactions on industry applications*, vol. 31, no. 4, pp. 802–811, 1995.
- [12] P. Choudhary, S. Dubey, and V. Gupta, "Efficiency optimization of induction motor drive at steady-state condition," in *2015 International Conference on Control, Instrumentation, Communication and Computational Technologies (ICCICCT)*. IEEE, 2015, pp. 470–475.
- [13] D. de Almeida Souza, W. C. de Aragao Filho, and G. C. D. Sousa, "Adaptive fuzzy controller for efficiency optimization of induction motors," *IEEE Transactions on Industrial Electronics*, vol. 54, no. 4, pp. 2157–2164, 2007.
- [14] B. Blanus, "New trends in efficiency optimization of induction motor drives," *New Trends in Technologies: Devices, Computer, Communication and Industrial Systems*, vol. 2, no. 11, p. 341, 2010.
- [15] Z. Qu, M. Ranta, M. Hinkkanen, and J. Luomi, "Loss-minimizing flux level control of induction motor drives," *IEEE Transactions on industry applications*, vol. 48, no. 3, pp. 952–961, 2012.
- [16] G. C. Sousa, B. K. Bose, and J. G. Cleland, "Fuzzy logic based on-line efficiency optimization control of an indirect vector-controlled induction motor drive," *IEEE Transactions on Industrial Electronics*, vol. 42, no. 2, pp. 192–198, 1995.
- [17] B. K. Bose, N. R. Patel, and K. Rajashekara, "A neuro-fuzzy-based on-line efficiency optimization control of a stator flux-oriented direct vector-controlled induction motor drive," *IEEE Transactions on Industrial Electronics*, vol. 44, no. 2, pp. 270–273, 1997.
- [18] C.-M. Ta and Y. Hori, "Convergence improvement of efficiency-optimization control of induction motor drives," *IEEE Transactions on Industry Applications*, vol. 37, no. 6, pp. 1746–1753, 2001.
- [19] S. Ameli and O. M. Anubi, "Robust control for a class of nonlinearly coupled hierarchical systems with actuator faults," *IFAC-PapersOnLine*, vol. 54, no. 20, pp. 540–546, 2021.
- [20] S. Maiti, C. Chakraborty, Y. Hori, and M. C. Ta, "Model reference adaptive controller-based rotor resistance and speed estimation techniques for vector controlled induction motor drive utilizing reactive power," *IEEE Transactions on industrial Electronics*, vol. 55, no. 2, pp. 594–601, 2008.
- [21] J. Guzinski and H. Abu-Rub, "Speed sensorless induction motor drive with predictive current controller," *IEEE Transactions on Industrial Electronics*, vol. 60, no. 2, pp. 699–709, 2012.
- [22] A. Balogun, O. Ojo, and F. Okafor, "Efficiency optimization of doubly-fed induction generator transitioning into shorted-stator mode for extended low wind speed application," in *IECON 2013 - 39th Annual Conference of the IEEE Industrial Electronics Society*, 2013, pp. 1601–1606.
- [23] P. C. Krause, O. Wasynczuk, S. D. Sudhoff, and S. D. Pekarek, *Analysis of electric machinery and drive systems*. John Wiley & Sons, 2013, vol. 75.
- [24] N. Mohan, *Advanced electric drives: analysis, control, and modeling using MATLAB/Simulink*. John Wiley & sons, 2014.
- [25] L. Yousfi, A. Bouchemha, M. Bechouat, and A. Boukrouche, "Vector control of induction machine using pi controller optimized by genetic algorithms," in *2014 16th International Power Electronics and Motion Control Conference and Exposition*. IEEE, 2014, pp. 1272–1277.
- [26] J. Amaral, R. Tanscheit, and M. Pacheco, "Tuning pid controllers through genetic algorithms," *complex systems*, vol. 2, no. 3, 2018.
- [27] D. Meena and A. Devanshu, "Genetic algorithm tuned pid controller for process control," in *2017 International Conference on Inventive Systems and Control (ICISC)*. IEEE, 2017, pp. 1–6.